Relative Configuration and Conformation of Key Intermediates for Matrix Metalloproteinase Inhibitors as Determined by NMR-Based Restrained Simulated Annealing and Validated by X-ray Analysis

Hans Matter,* Martin Knauf, Wilfried Schwab, and Erich F. Paulus

Hoechst Marion Roussel
Core Research Functions & Chemical Research
D-65926 Frankfurt am Main, Germany

Received July 9, 1998
Revised Manuscript Received September 8, 1998

The information about relative and absolute configuration of stereogenic centers in natural products and synthetic key intermediates is indispensable for modern medicinal chemistry. To achieve spatial complementarity between ligands and specific target enzymes, an understanding of stereoselective transformations is required. Here we describe the application of a strategy to simultaneously determine configuration and conformation of key intermediates in the synthesis of enzyme inhibitors using 2D NMR spectroscopy and simulated annealing[1] including a floating chirality approach.[2]

Since matrix metalloproteinases are of growing interest in pharmaceutical research,[3] we have investigated key intermediates for stromelysin (MMP-3) inhibitors with S1′ directed biphenylsulfonyl side chains.[4] Their relative configurations were unambiguously obtained using this approach and could be validated using X-ray structure analysis. To our knowledge, this is the first example of this strategy combined with an independent validation showing its potential to rapidly obtain relevant stereochemical information.[5]

The synthetic route (cf. Figure 1) started from (*R*)-tetrahydroisoquinolin-3-carboxylate **1**, which was N-sulfonated.[6] **2** was converted to the aldehyde **4** by reduction to **3** using BMS[7] and oxidation using *o*-iodoxybenzoic acid IBX.[8] The loss of optical rotation from **3** to **4** indicates racemization despite the extremely mild conditions. Due to lack of stability, **4** was directly converted to the configurationally stable *N*-methylnitrone **5**. Heating a solution of **5** resulted in 1,3-dipolar cycloaddition to give the desired isoxazolidines **6** in a 48.6:51.4 ratio of **6a** (*RSS*/*SRR*, trans) and **6b** (*RSR*/*SRS*, cis). The low cis/trans stereoselectivity has been overcome in special cases.[9] The stereodirecting effect of α-chiral nitrones during olefin cycloaddition was described using different transition state models.[10] Our data suggest that cycloaddition of tetrahydroisoquinolin nitrones preferably results in 4*R*/3*S* (4*S*/3*R*) stereochemistry.

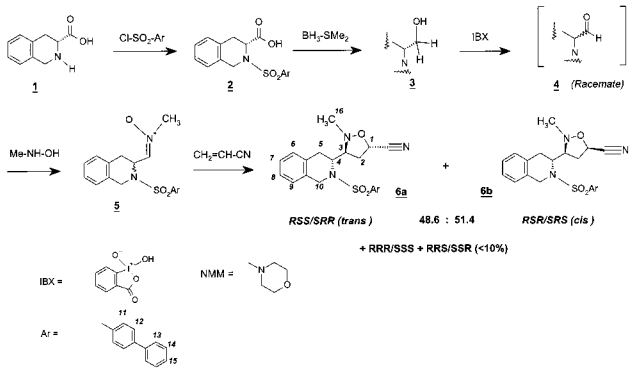

Figure 1. Synthesis of both diastereomeric MMP-3 inhibitor key intermediates **6a** and **6b**.

After the assignment of ^{1}H NMR resonances[11] for **6a** and **6b** (cf. Supporting Information), distance constraints were extracted from 2D NOESY and ROESY spectra by conversion of cross-peak volumes into interproton distances using the isolated spin pair approximation (ISPA). Thirty-one and 26 nontrivial distance constraints were obtained for **6a** and **6b**, respectively.[12] In addition, homonuclear *J*-coupling constants (cf. Supporting Information) were converted into dihedral angle information.[13] For both compounds the NMR spectra indicate the existence of a single preferred conformation.[14]

The NOE restrained simulated annealing calculations[1] were performed using SYBYL.[15,16] Since it is not possible to determine absolute configurations in distance space, carbon C4 was set to *R*-chirality. Thus, four different starting configurations for carbons C4, C3, and C1 (*RSS*, *RSR*, *RRS*, and *RRR*) were considered for each intermediate. The NMR-derived distance constraints were applied as a biharmonical function. An energetic force field was used where experimentally derived distance constraints have higher force constants than the terms maintaining individual atom chiralities. Thus, chiral centers are allowed to invert during the simulation. For each starting configurations, 50 structures were calculated, which were all combined for analysis yielding 200 individual structures for **6a** and **6b**,[17] respectively.

Acceptable structures were selected on the basis of the maximum pairwise rmsd violations[18] as objective criteria. For each structure, the maximum rmsd to all structures with lower

* To whom the correspondence should be addressed. Phone: ++49-69-305-84329. Fax: ++49-69-331399. E-mail: hans.matter@hmrag.com.

(1) Nilges, M.; Clore, G. M.; Gronenborn, A. M. *FEBS Lett.* **1988**, *229*, 317−324.

(2) Weber, P. L.; Morrison, R.; Hare, D. *J. Mol. Biol.* **1988**, *3*, 483−487.

(3) (a) Zask, A.; Levin, J. I.; Killar, L. M.; Skotnicki, J. S. *Curr. Pharm. Des.* **1996**, *2*, 624−661. (b) Hagmann, W. K.; Lark, M. W.; Becker, J. W. *Ann. Rep. Med. Chem.* **1996**, 231−240. (c) Ye, Q. Z.; Hupe, D.; Johnson, L. *Curr. Med. Chem.* **1996**, *3*, 407−418.

(4) Esser, C. K.; Bugianesi, R. L.; Caldwell, C. G.; Chapman, K. T.; Durette, P. L.; Girotra, N. N.; Kopka, I. E.; Lanza, T. J.; Levorse, D. A.; MacCoss, M.; Owens, K. A.; Ponpipom, M. M.; Simeone, J. P.; Harrison, R. K.; Niedzwiecki, L.; Becker, J. W.; Marcy, A. I.; Axel, M. G.; Christen, A. J.; McDonnell, J.; Moore, V. L.; Olszewski, J. M.; Saphos, C.; Visco, D. M.; Shen, F.; Colletti, A.; Krieter, P. A.; Hagmann, W. K. *J. Med. Chem.* **1997**, *40*, 1026−1040.

(5) For a pioneering approach, see: Reggelin, M.; Hoffmann, H.; Köck, M.; Mierke, D. F. *J. Am. Chem. Soc.* **1992**, *114*, 3272−3277.

(6) Experimental conditions, see Supporting Information.

(7) Lane, C. F. *Aldrichim. Acta* **1977**, *10*, 41−51.

(8) (a) Frigerio, M.; Santagostino, M.; Sputore, S.; Palmisano, G. *J. Org. Chem.* **1995**, *60*, 7271−7276. (b) Plumb, J. B.; Harper, D. J. *Chem. Eng. News* **1990**, 3.

(9) Mukai, C.; Kim, I. J.; Cho, W. J.; Kido, M.; Hanaoka, M. *J. Chem. Soc., Perkin Trans. 1* **1993**, 2494−2503.

(10) (a) Vasella, A.; Voeffray, R. *Helv. Chim. Acta* **1982**, *65*, 1134−1144. (b) DeShong, P.; Li, W.; Kennington, J. W.; Ammon, H. L. *J. Org. Chem.* **1991**, *56*, 1364−1373. (c) Baggiolino, E. G.; Iacobelli, J. A.; Hennessy, B. M.; Batcho, A. D.; Sereno, J. F.; Uskokovic, M. R. *J. Org. Chem.* **1986**, *51*, 3098−3108.

(11) NMR samples were prepared by dissolving **6a** and **6b** in 0.6 mL of $CDCl_3$. NMR spectra were obtained in the phase sensitive mode on a BRUKER DRX 600 spectrometer at 300 K using TPPI for quadrature detection in F_1. For ROESY experiments, a mixing time of 150 ms was used for both epimers. The mixing times for the NOESY experiments of **6a** and **6b** were set to 600 ms and 1 s, respectively.

(12) For nondiastereotopically assigned CH_2 protons and methyl groups, 90 and 100 pm were added to the upper bounds as pseudoatom corrections (Wüthrich, K. *NMR of Proteins and Nucleic Acids*; Wiley: New York, 1986). Upper and lower limits have been set to ±10% of the calculated distances.

(13) A Karplus-type of equation (Karplus, M. *J. Chem. Phys.* **1959**, *30*, 11−15) with the following parameters was used: $A = 9.5$, $B = -1.6$, $C = 1.8$ (DeMarco, A.; Llinas, M.; Wüthrich, K. *Biopolymers* **1978**, *17*, 617−636).

(14) The diastereotopic protons show significant chemical shift differences and different vicinal coupling constants. The line shapes of the resonance signals do not indicate any conformational heterogeneity (Kessler, H. *Angew. Chem., Int. Ed. Engl.* **1982**, *21*, 512−523).

(15) SYBYL Molecular Modelling Package, Versions 6.3, Tripos, St. Louis, MO, 1996.

(16) All energy calculations were based on the TRIPOS 6.0 force field (Clark, M.; Cramer, R. D., III; Van Opdenbosch, N. *J. Comput. Chem.* **1989**, *10*, 982−1912) including Gasteiger−Marsili charges (Gasteiger, J.; Marsili, M. *Tetrahedron* **1980**, *36*, 3219−3228).

10.1021/ja982415e CCC: $15.00
Published on Web 10/27/1998

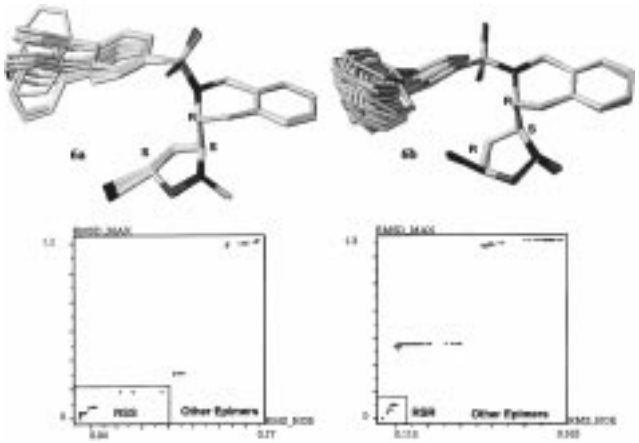

Figure 2. Results of the NMR-based analysis of both epimers. In the upper left panel, the conformational ensemble of 20 acceptable structures for **6a** (*RSS* chirality) is given. In the lower left panel, the maximum of the rms deviation is shown between pairs of conformers with a rms NOE violation smaller than a cutoff value as objective criterium for ensemble selection. The sample of structures for rms deviation gets progressively larger with increasing cutoff values for the NOE violation, as plotted on the *x*-axis. On the *y*-axis, the maximum rms deviation values are given. In the upper right part, the ensemble of 28 acceptable structures for diastereomer **6b** (*RSR* chirality) is shown in combination with the corresponding maximum rmsd graph (lower right panel).

constraint violations was plotted on the *y*-axis as a function of the constraint violation (Figure 2, lower panel). For a conformer family, the maximum rmsd raises continuously as a function of the violation of the experimental data. However the scatter plots in Figure 2 reveal significant steps, indicating that new conformational and/or configuration states become accessible, which differ significantly from all structures with lower violations. These plateaus with higher violations and rmsd values correspond to alternative configurations at carbons C1 and/or C3.

For **6a**, 69 structures with low NOE violations are acceptable. All reveal *RSS* chirality at C4, C3, and C1 (Figure 2, box in lower panel). Interestingly, 40% of those structures were obtained from different starting configurations by inversion of chiral centers. In fact, the structure with the lowest NOE violation results from an *RSR* starting diastereomer. In contrast, all diastereomers starting with *RSS* maintain their chiralities. For analysis, the first well-defined plateaus in Figure 2 (left) with rms NOE violations between 0.03 and 0.04 Å were considered, leading to 20 representative structures for **6a** (Figure 2, upper left panel). The second plateau for **6a** with 49 conformers also corresponds to *RSS* configurations but now represents another conformational state characterized by a different orientation of the biphenyl moiety.

The same analysis for **6b** revealed the *RSR* configuration at C4, C3, and C1. Again, no chirality inversion was observed for the *RSR* starting structures. The most acceptable 28 conformers and the maximum rmsd plots are displayed in Figure 2 on the right.

All NOE-derived constraints are fulfilled for both epimers (cf. Supporting Information). Only one NOE in the biphenyl residue

(17) A time step of 1.0 fs was used for the integration of Newton's equation of motion for a duration of 200 ps each. The kinetic energy was included by coupling the system to a thermal bath (Berendsen, H. J. C.; Postma, J. P. M.; van Gunsteren, W. F.; Di Nola, A.; Haak, J. R. *J. Chem. Phys.* **1984**, *81*, 3684−3690). The atomic velocities were applied following a Boltzmann distribution about the center of mass to obtain a starting temperature of 1000 K. The force constants for upper and lower boundaries were initially set to 50 kcal/mol·Å^2. After simulating for 1.5 ps at 1000 K, the system temperature was stepwise reduced using an exponential function over a 2.5 ps period to reach a final temperature of 200 K. Resulting structures were sampled every 4 ps and minimized resulting a protocol of 50 cycles with 4 ps simulation time for each of the 4 starting isomers. The total CPU time per diastereomer (200 structures) was approximately 3 h. per diastereomer (200 structures) was approximately 3 h.

(18) Widmer, H.; Widmer, A.; Braun, W. *J. Biomol. NMR* **1993**, *3*, 307−324.

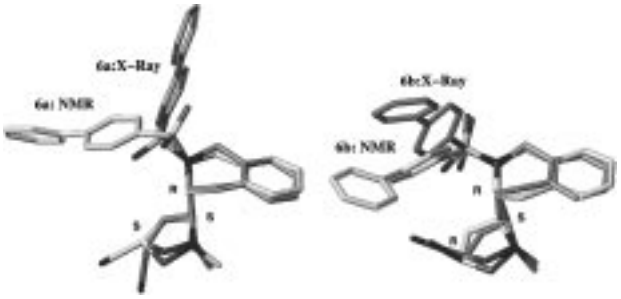

Figure 3. Comparison between representative solution structures (white carbon atoms) and solid-state structures (grey carbon atoms) for diastereomers **6a** (left) and **6b** (right).

for epimer **6a** is slightly violated by 0.11 Å (averaged over 20 conformers). A similar agreement is observed for the second epimer **6b**, although the resonance overlap of protons H2, H3, and H5 led to a higher uncertainty in the NOE distance restraints, causing a higher NOE violation for all 28 *RSR* conformers.

For **6a**, strong NOE between H1 and H4 and a weaker correlation for H1 and H3 count for a H1−H3 trans orientation. However, the full differentiation between all possible stereoisomers at C4, C3, and C1 could only be achieved in a straightforward manner using this combined experimental and computational approach. The situation was even more difficult for **6b** since no unambiguous NOE effects between protons H1−H4 and H1−H3 were observed, whereas the calculation unambiguously led to the *RSR* diastereomer with a cis orientation of H1 and H3.

Subsequently an X-ray structure analysis[19] for validation confirmed the relative configurations for both epimers obtained by NMR. The comparison between solid state and solution structures for **6a** and **6b** is displayed in Figure 3. The only remarkable difference between solution and solid-state structures is the orientation of the biphenyl moiety in both epimers, which might result from crystal packing effects. Concerning the heterocyclic system, conformations and distances are very similar.

This validated approach for the simultaneous determination of conformation and configuration rapidly and efficiently deduces the correct relative stereochemistry. As earlier proposed,[5] force field modifications allowing chiral centers to convert produce configurations consistent with all experimental data. The unbiased structure analysis based on NOE rms violation of individual conformers unambiguously allows the selection of acceptable structures in accord with experimental data. For further testing during implementation of this strategy, compound **1** of reference 5 was used, leading to identical results as described therein. Thus, our results clearly demonstrate the potential of this powerful approach to obtain relevant information in a timely and straightforward manner.

Acknowledgment. The work of Holger Thiel during the synthesis of the herein described molecules is gratefully acknowledged.

Supporting Information Available: Experimental conditions and four additional tables with ^{1}H chemical shifts, homonuclear experimental and backcalculated ^3J(H,H) coupling constants, and experimentally derived distance constraints in comparison to computed averaged distances for **6a** and **6b** (5 pages, print/PDF). See any current masthead page for ordering information and Web access instructions.

JA982415E

(19) Experimental conditions, see Supporting Information. Paulus, E. F.; Schwab, W.; Knauf, M.; Matter, H. 1998, in preparation.